Wiley Online Library
Early View publication on www.wileyonlinelibrary.com
(issue and page numbers not yet assigned;
citable using Digital Object Identifier – DOI)

Phys. Status Solidi RRL, 1–5 (2016) / DOI 10.1002/pssr.201600059

pss +++rapid research letters+++
www.pss-rapid.com

Impact of surface recombination on efficiency of III-nitride light-emitting diodes

Kirill A. Bulashevich and Sergey Yu. Karpov*

STR Group – Soft-Impact, Ltd., P.O. Box 83, 27 Engels av., 194156 St. Petersburg, Russia

Received 29 February 2016, accepted 6 April 2016
Published online 11 April 2016

Keywords surface recombination, efficiency, nitrides, light-emitting diodes, InGaN, chip design, simulation

* Corresponding author: e-mail sergey.karpov@str-soft.com, Phone: +7 812 554 4570, Fax: +7 812 326 6194

The paper considers surface recombination at the free active region surface as the mechanism of carrier losses which has not yet been discussed with regard to III-nitride LEDs despite of its evident importance for AlGaInP-based light emitters. Using advanced thin-film and triangular volumetric chip designs reported in literature as prototypes, we have demonstrated by simulation a noticeable impact of surface recombination on the wall-plug efficiency of InGaN-based LEDs. Various types of LEDs whose efficiency may be especially affected by surface recombination are discussed.

1 Introduction Surface recombination is known as an important channel of carrier losses in AlGaInP-based LEDs. Detailed study of square-mesa micro-cavity red LEDs has demonstrated surface recombination to affect noticeably the LED emission efficiency at the mesa size of ~250 μm and smaller [1]. In contrast, surface recombination have not been ever considered as the valuable factor limiting efficiency of state-of-the-art blue and green III-nitride LEDs. Partly, this was caused by a relatively low surface recombination velocities (SRVs) reported for GaN and InGaN, as compared to those of zinc-blende semiconductors. Figure 1 summarizes the data on measured SRVs in various III–V semiconductors borrowed from [2–9] and references therein. There are two major trends seen from the figure: SRV (i) decreases with the materials bandgap and (ii) increases in the In → Ga → Al anion row. It should be also noted that the data on zinc-blende semiconductors in Fig. 1 pertain mainly to the (001) surface orientation. In GaN, however, SRVs related to (0001) and (000 $\bar{1}$) facets may differ by 2–3 orders of magnitude, reaching the value as high as ~10^6 cm/s [6]. In the case of (0001) LED structures, the most important planes that may contribute to surface recombination are non-polar ones. The corresponding SRV values reported for InGaN range from ~3×10^2 [5] to ~10^4 cm/s [7], depending on surface preparation and treatment (epitaxial growth or ion etching). So, the point corresponding to InGaN in Fig. 1 indicates the SRV value averaged over all possible surface orientations. In general, however, the experimental SRVs of nitride semiconductors should be yet regarded as largely uncertain, requiring more elaborated evaluation in future.

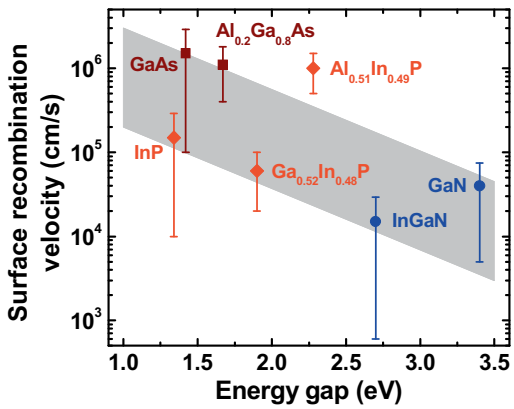

Figure 1 Experimental SRVs of selected III–V semiconductors compiled from various sources. Bars show the ranges of the reported values, whereas symbols indicate the most frequent/averaged ones. Grey shadow demonstrates a general trend of the surface recombination velocity variation with the materials bandgap.

Except for SRV, another important parameter controlling surface recombination impact on the LED efficiency is the length of carrier diffusion in the LED active region, being dependent on both carrier diffusivity and lifetime. From this point of view, phosphide and nitride materials also differ substantially. First, due to a wider bandgap and composition fluctuations, the ambipolar diffusion coefficients (ADCs) in InGaN alloys are an order of magnitude smaller than in conventional zinc-blende semiconductors. Second, nitride LEDs operate at non-equilibrium carrier concentrations much higher than phosphide LEDs, which results in considerably shorter carrier lifetime. All this provides considerably smaller carrier diffusion lengths in the active regions of III-nitride LEDs, as compared to those in phosphide ones.

Both lower SRVs and smaller carrier diffusion lengths suggest that surface recombination may be withdrawn from the mechanisms limiting efficiency of III-nitride LEDs. In this paper, we will show, however, that it is not the case. Because of lacking experimental data on this issue, we have used numerical simulations in order to clarify the possible impact of surface recombination on the LED efficiency.

2 Model In order to address complex realistic geometries of state-of-the-art LEDs, we have applied the hybrid approach to model LED operation, combining 3D simulation of the current spreading and heat transfer in the LED die with 1D analysis of carrier injection and their recombination in the LED active region [10]. To account for the lateral carrier transport in the active region we consider sheet electron n and hole p concentrations obeyed the steady-state 2D continuity equations

$$\nabla\cdot\mathbf{J}_\mathrm{n}=\frac{j\eta_\mathrm{inj}}{q}-R(n,p)\,,\qquad \nabla\cdot\mathbf{J}_\mathrm{p}=\frac{j\eta_\mathrm{inj}}{q}-R(n,p)\,, \tag{1}$$

where q is the elementary charge, R is the recombination rate, j is the local vertical current density, η_inj is the injection efficiency defined as the ratio of the recombination current density in the active region to j, and $\mathbf{J}_\mathrm{n}$ and $\mathbf{J}_\mathrm{p}$ are the lateral electron and hole fluxes, respectively, defined as

$$\mathbf{J}_\mathrm{n}=-\mu_\mathrm{n} n\,\mathbf{E}-D_\mathrm{n}\,\nabla n\,,\qquad \mathbf{J}_\mathrm{p}=\mu_\mathrm{p} p\,\mathbf{E}-D_\mathrm{p}\,\nabla p\,. \tag{2}$$

Here, $\mathbf{E}$ is the in-plane electric field and $\mu_{\mathrm{n,p}}$ and $D_{\mathrm{n,p}}$ are, respectively, the mobilities and diffusion coefficients of electrons/holes in the active region.

Subtracting one of Eq. (1) from another, one can obtain that $\mathbf{J}_\mathrm{n}=\mathbf{J}_\mathrm{p}=\mathbf{J}$; excluding then electric field $\mathbf{E}$ from Eq. (2), one can derive the expression for the carrier flux

$$\mathbf{J}=-\frac{D_\mathrm{n}\mu_\mathrm{p} p\;\nabla n+D_\mathrm{p}\mu_\mathrm{n} n\;\nabla p}{\mu_\mathrm{n} n+\mu_\mathrm{p} p}\,. \tag{3}$$

In terms of new variables, $N=(np)^{1/2}$ and $r=(n/p)^{1/2}$ the above expression for the flux $\mathbf{J}$ can be written as

$$\mathbf{J}=-\frac{D_\mathrm{n}\mu_\mathrm{p}+D_\mathrm{p}\mu_\mathrm{n}}{\mu_\mathrm{n} r+\mu_\mathrm{p}/r}\nabla N-\frac{D_\mathrm{n}\mu_\mathrm{p}-D_\mathrm{p}\mu_\mathrm{n}}{\mu_\mathrm{n} r+\mu_\mathrm{p}/r}\left(N\frac{\nabla r}{r}\right). \tag{4}$$

The second term in Eq. (4) vanishes, if (i) electrons and holes are non-degenerated, so that $D_{\mathrm{n,p}}=(kT/q)\mu_{\mathrm{n,p}}$, where k is the Boltzmann constant and T is temperature, or (ii) $\nabla N/N\gg\nabla r/r$ (in particular case of electrically neutral active region, $r=1$). Simulations show that the latter requirement is practically always met in the case of III-nitride LEDs. Therefore, the second term in Eq. (4) can be omitted. Inserting the reduced expression (4) into Eq. (1), one can obtain the governing equation

$$\begin{aligned}&\nabla(D_\mathrm{a}\,\nabla N)=R(N,r)-\frac{j\eta_\mathrm{inj}}{q}\,,\\&D_\mathrm{a}=\frac{D_\mathrm{n}\mu_\mathrm{p}+D_\mathrm{p}\mu_\mathrm{n}}{\mu_\mathrm{n} r+\mu_\mathrm{p}/r}\,,\end{aligned} \tag{5}$$

where D_a is the ADC of carriers in the active region. This equation is supplemented with the boundary conditions $\boldsymbol{\nu}\cdot\mathbf{J}=SN$ with $\boldsymbol{\nu}$ being the outer normal to the active region perimeter and S being SRV generally dependent on r. Equation (5) should be solved numerically with j, η_inj, and $R(N,r)$ distributions over the active region found from the hybrid 3D/1D simulations [10].

3 Results We consider here two representative LED chip designs. One is similar to unpackaged blue-LED thin-film chip described in Ref. [11]. In this chip, silver-based electrodes are formed to the p-contact layer of an LED structure; after removing the sapphire substrate the back surface of the n-contact layer is textured to increase the efficiency of light extraction from the LED, and the current access to the n-contact layer is provided by metallic column electrodes passing through blind vias etched through the structure up to the n-contact layer (see [11] and references therein for more details). Because of current crowding around the vias, we expect to see a noticeable impact of surface recombination on the LED efficiency despite a relatively small total perimeter of all the vias.

Another representative chip design is similar to packaged violet-LED triangular volumetric chip reported in [12]. No substantial current crowding is expected in this kind of chip but the perimeter of the active region free surface is here large enough to expect surface recombination affecting the LED efficiency.

As the LED structures used in the above chips were not disclosed, the 1D simulations of carrier injection and recombination in the active regions were substituted by fitting the experimental current–voltage and light-current characteristics, using the Shockley's diode equation accounting for LED series resistance and the ABC-recombination model [13], respectively. In order to dimin-

ish uncertainty in the fitting parameters, experimental recombination coefficients reported in [14] were utilized. 3D modelling of current spreading in the LED dice was carried out with commercial SimuLED package [15], assuming isothermal operation conditions for simplicity.

According to [16–18], ADCs of carriers in InGaN QWs depend on the alloy composition, materials quality, and non-equilibrium carrier concentration, generally ranging from 0.2 to 3.0 cm^2/s. In this study, we used its representative value of 2.0 cm^2/s corresponding to a relative high carrier concentrations [17]. Because of the uncertainty in the SRVs reported for InGaN, we have varied its value from zero (no surface recombination) to 3×10^5 cm/s.

Figure 2 shows simulated wall-plug efficiencies (WPEs) of the considered LED chips as a function of operating current. One can see that surface recombination reduces maximum WPE values by ~5–7 absolute percent in both types of the chip, depening on the SRV assumed. It is interesting that the impact of surface recombination becomes practically independent of SRV at $S > 10^4$ cm/s. At the operating currents much greater than those corresponding to the WPE maxima, the surface recombination effect becomes much weaker. In order to understand the influence

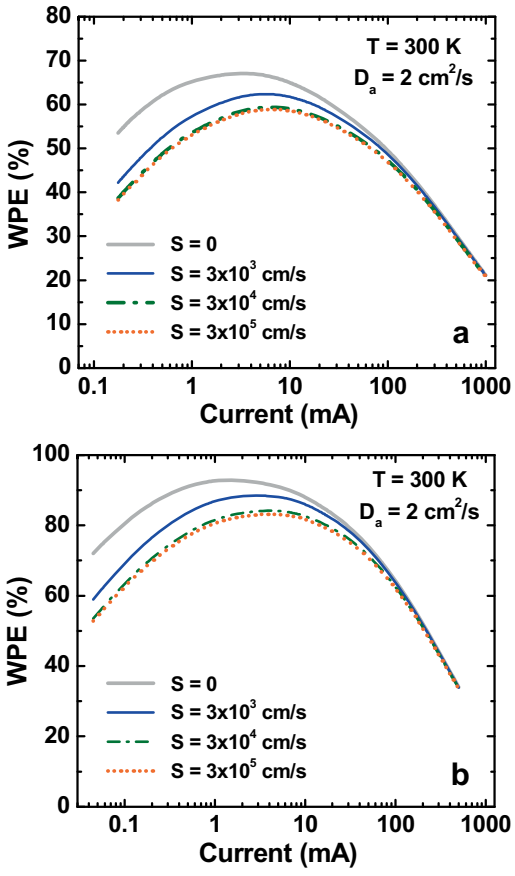

Figure 2 Wall-plug efficiency of the unpackaged thin-film blue LED (a) and packaged triangular volumetric violet LED (b) chips as a function of operating current simulated at different values of SRV from zero to 3×10^5 cm/s.

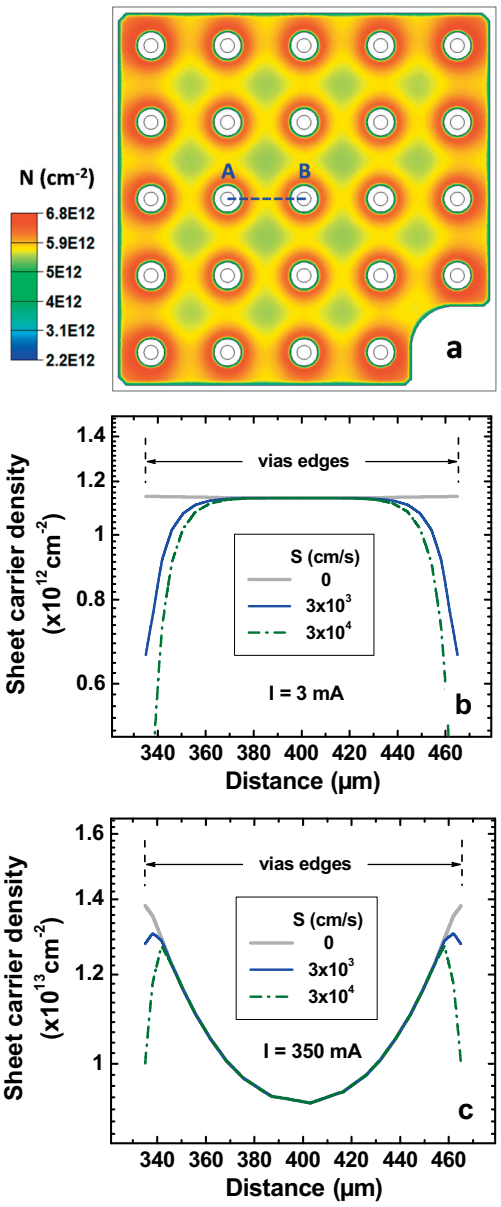

Figure 3 Distribution of sheet carrier density N over the active region of the thin-film LED chip at the operating current of 100 mA and $S = 3 \times 10^4$ cm/s (a) and such distributions in the cross-section AB computed for the currents of 3 mA (b) and 350 mA (c) at different SRV values.

of the operating current on the strength of surface recombination effect, we have plotted in Fig. 3 the two-dimensional distribution of the sheet carrier density N in the active region at the operating current of 100 mA (Fig. 3a), and distributions of N between two selected vias placed at the center of the thin-film LED chip (AB cross-section), simulated for the current of 3 mA nearly corresponding to the WPE maximum (Fig. 3b) and for much higher current of 350 mA (Fig. 3c). At low currents (3 mA) and negligible surface recombination ($S = 0$), the carrier density is quite uniform, demonstrating the absence of

visible current crowding. Surface recombination leads to formation around the vias a dead region depleted with carriers where they outcome from to recombine non-radiatively on the free active region surface. The width of the region of ~20–25 μm corresponds to the carrier ambipolar diffusion length at a rather long life time specific for the low carrier density of ~10^{12} cm^{-2}.

At the currents as high, as ~100 mA, the sheet carrier density becomes no longer uniformly distributed over the active region (Fig. 3a) because of current crowding. At 350 mA, a strong non-uniformity is predicted even in the absence of surface recombination (see Fig. 3c). Similarly to the low-current case, surface recombination forms dead regions around the vias. However, the width of the region is now of ~5–8 μm, corresponding to the diffusion length at a much shorter carrier life time specific for the higher carrier density of ~10^{13} cm^{-2}. In addition, the contrast of the carrier density distribution, i.e. the ratio of the carrier density at the vias edges to its maximum value, also becomes lower at high currents. Both the lower carrier density contrast and the narrower dead region result in a weaker impact of surface recombination on the LED efficiency at high currents.

4 Discussion Our simulations demonstrate surface recombination to be capable of influencing noticeably the efficiency of state-of-the-art violet and blue LEDs, especially at low operating currents. Though the predicted effect is weaker than in the case of AlGaInP LEDs, its impact on the efficiency is, nevertheless, tangible in view of the common wish to achieve the ultimate performance of III-nitride light emitters. Being largely dependent of the chip size, the impact of surface recombination on the efficiency is expected to be especially pronounced in micro-LEDs, multi-pixel LED arrays, nanostructure LEDs, and some kinds of ridge-waveguide laser diode.

Dependence of surface recombination strength on the LED emission wavelength is beyond the scope of this study. Nevertheless, accounting for general trend of reducing ADC in InGaN QWs with the In content [17], we can forecast suppression of surface recombination in green LEDs and its enhancement in violet LEDs, as compared to blue ones (this effect has not been accounted for in the present simulations). Even more stronger should be the surface recombination impact on the efficiency in near- and deep-UV LEDs because of (i) a pronounced tendency of the devices to current crowding, (ii) general trend of increasing SRV with the Al content in the active region, and (iii) higher carrier diffusivity which is no longer controlled by strong composition fluctuations typical for InGaN alloys.

In any case, passivation of free active region surface with appropriate dielectrics may help to diminish the negative impact of surface recombination on the LED efficiency.

5 Conclusion A way of accounting for surface recombination impact on LED operation within hybrid 3D/1D modelling approach has been suggested in the paper. As the approach was developed for accelerated simulations of coupled current spreading and heat transfer in LED dice, the extension of the surface recombination model to non-isothermal operation conditions is straightforward.

Considering two advanced chip designs, we have shown by simulations that surface recombination may produce a noticeable impact on the efficiency of state-of-the-art blue and violet LEDs, reducing the maximum WPE values by about 5–7 absolute percent. At high operation currents, the impact of surface recombination becomes weaker due to a shorter carrier life time in the active region, resulting eventually in a smaller ambipolar carrier diffusion length.

The results obtained demonstrate still existing additional room for performance improvement of state-of-the-art visible LEDs and point out the importance of surface-recombination losses for light emitters with a large active region perimeter-to-area ratio, like micro-LEDs, multi-pixel LED arrays, nanostructure LEDs, etc. Additional enhancement of surface recombination impact on the LED efficiency is expected for UV LEDs.

Acknowledgements This study has been supported by European Union FP7, NEWLED project, grant number 318388.

References

[1] P. Royo, R. P. Stanley, M. Ilegems, K. Streubel, and K. H. Gulden, J. Appl. Phys. **91**, 2563 (2002).
[2] C. A. Hoffman, H. J. Gerritsen, and A. V. Nurmikko, J. Appl. Phys. **51**, 1603 (1980).
[3] M. Boroditsky, I. Gontijo, M. Jackson, R. Vrijen, E. Yablonovitch, T. Krauss, R. Bhat, and M. Krames, J. Appl. Phys. **87**, 3497 (2000).
[4] V. Ramesh, A. Kikuchi, K. Kishino, M. Funato, and Y. Kawakami, J. Appl. Phys. **107**, 114303 (2010).
[5] H. Kitagawa,. M. Fujita, T. Suto, T. Asano, and S. Noda, Appl. Phys. Lett. **98**, 181104 (2011).
[6] T. Onuma, N. Sakai, T. Igaki, T. Yamaguchi, A. A. Yamaguchi, and T. Honda, J. Appl. Phys. **112**, 063509 (2012).
[7] S. Zhang, Y. Li, S. Fathololoumi, H. P. T. Nguyen, Q. Wang, Z. Mi, Q. Li, and G. T. Wang, AIP Advances **3**, 082103 (2013).
[8] Y.-C. Leem, H.-M. Lee, Y.-S. Park, S.-Y. Yim, H. Jeong, G.-Y. Jung, and S.-J. Park, ECS J. Solid State Sci. Technol. **3**, Q153 (2014).
[9] Database of materials properties collected at the web site of the Ioffe Institute RAS: http://www.matprop.ru/
[10] K. A. Bulashevich, V. F. Mymrin, S. Yu. Karpov, I. A. Zhmakin, and A. I. Zhmakin, J. Comput. Phys. **213**, 214 (2006).
[11] I. E. Titkov, S. Yu. Karpov, A. Yadav, V. L. Zerova, M. Zulonas, B. Galler, M. Strassburg, I. Pietzonka, H.-J. Lugauer, and E. U. Rafailov, Appl. Phys. Lett. **50**, 911 (2014).
[12] C. A. Hurni, A. David, M. J. Cich, R. I. Aldaz, B. Ellis, K. Huang, A. Tyagi, R. A. DeLille, M. D. Craven, F. M. Steranka, and M. R. Krames, IEEE J. Quantum Electron. **106**, 031101 (2015).

[13] S. Yu. Karpov, Opt. Quantum Electron. **47**, 1293 (2015).
[14] D. Schiavon, M. Binder, M. Peter, B. Galler, P. Drechsel, and F. Scholz, Phys. Status Solidi B **250**, 283 (2013).
[15] http://www.str-soft.com/products/SimuLED/index.htm
[16] H.-C. Wang, S.-W. Feng, T. Malinauskas, K. Jarašiunas, C. C. Ting, S. Liu, and C.-Y. Tsai, Thin Solid Films **518**, 7291 (2010).
[17] J. Danhof, H.-M. Solowan, U. T. Schwarz, A. Kaneta, Y. Kawakami, D. Schiavon, T. Meyer, and M. Peter, Phys. Status Solidi B **249**, 480 (2012).
[18] R. Aleksiejūnas, K. Gelžinytė, S. Nargelas, K. Jarašiūnas, M. Vengris, E. A. Armour, D. P. Byrnes, R. A. Arif, S. M. Lee, and G. D. Papasouliotis, Appl. Phys. Lett. **104**, 022114 (2014).